



Theoretical structure prediction of TcaA from *Photorhabdus luminescens* and aminopeptidase N receptor from *Helicoverpa armigera*

Maithri S.K., Ramesh K.V.* and Mutangana Dieudonné

Department of Biotechnology, Center for Postgraduate studies, Jain University, Jayanagar, Bangalore – 560011, INDIA

Available online at: www.isca.in

Received 12th October 2012, revised 22nd November 2012, accepted 22nd December 2012

Abstract

Due to resistance developed by various agricultural pests towards *Bacillus thuringiensis* (BT) toxins, there is a necessity of developing alternative biopesticide. The TcaA toxin produced by *Photorhabdus luminescens* is a high molecular weight insecticidal toxin having toxicity against wide range of agricultural pests. Phylogenetic tree constructed for TcaA revealed that this toxin does not have any ancestral relationship with BT toxins. Present study focused on the modeling the TcaA toxin from *Photorhabdus luminescens* and aminopeptidase N receptor from *Helicoverpa armigera* using various computational approaches. Structural validation using various tools such as ProSA and PROCHECK revealed that Φ and ψ angles of these theoretical models were present in the core and allowed region. The theoretical toxin structure was subsequently docked onto the homology modeled aminopeptidase N receptor. Outcome of the docking study showed that first domain of TcaA had highest docking energy when compared to remaining domains.

Keywords: TcaA, APN, docking, molecular modelling, domain.

Introduction

Various problems are associated with the application of synthetic insecticides. Many of these insecticides are non-biodegradable, undergo slow degradation and persist in the environment for a long time. Also excessive and prolonged uses of synthetic insecticides can lead to the development of insect resistance¹. To overcome the environmental hazards caused by the application of synthetic insecticides, biopesticides offer a better alternative. For instance, *Bacillus thuringiensis* accounts for 90% of the bio insecticide market; it produces insecticidal toxins called delta endotoxins (BT toxin) which are proteinaceous, readily biodegradable and also have a short half-life inside the insect midgut². In the recent past, many of the crop pests have developed resistance towards BT toxins and this includes: *Ostrinia nubilalis* (European corn borer), *Heliothis virescens* (Tobacco bud worm), *Pectonophora gossypiella* (Pink bollworm moth), *Culex quinquefasciatus* (Mosquito), *Aedes aegypti* (Yellow fever mosquito), *Trichloro plusiani* (Tiger moth), *Leptinotarsa decemlineata* (Colorado potato beetle), *Spodoptera exigua* (Beet armyworm), *Spodoptera littoralis* (Egyptian cotton leaf worm), and *Chrysomela scripta* (Cottonwood leaf beetle)³⁻⁷. Therefore, insecticidal toxins of *Photorhabdus luminescens* can be considered as a potential substitute to the BT toxin.

Photorhabdus luminescens is a gram-negative entomopathogenic enterobacterium that exists in mutualistic symbiosis with nematodes of the family *Heterorhabditidae* found in the gut of infective insect host *Heterorhabditis bacteriophora*⁸. After entering inside the insect host, the nematode releases the bacteria by regurgitation directly into the

insect's hemocoel. In the hemocoel, these bacteria replicate rapidly and cause lethal sepsis by producing different high molecular weight toxins that kill the insect within 48–72 hours⁹. Among various insecticidal toxins produced by the *Photorhabdus luminescens* purified TcaA was shown to disrupt the insect midgut epithelium in a manner similar to the δ -endotoxins from *Bacillus thuringiensis*⁸.

There are several studies reporting that glycosyl-phosphatidylinositol (GPI) anchored aminopeptidase N (APN)¹⁰ and cadherin-like protein¹¹ of *Manduca sexta* act as receptors for the BT toxins. Among these two receptors, the APN receptor belongs to the Zn-binding metalloprotease family. The C-terminal region of the APN binding site is rich in N-acetylgalactosamine (GalNAc) and acts as the binding site of the Cry1Ac toxin^{10,12}.

Although the toxin protein produced by *Photorhabdus* bacterium has been proved to be toxic against wide variety of insects⁸, structural information of these proteins is yet to be resolved through X-ray / NMR experiments. Therefore in the present study we report 3D models for TcaA toxin (*Photorhabdus luminescens* w14) as well as APN receptor (*Helicoverpa armigera*). Further we have also examined the molecular interaction of TcaA toxin with the APN receptor through the docking studies.

Material and Methods

Phylogenetic analysis: Amino acid sequence of TcaA from *Photorhabdus luminescens* in FASTA format along with the insecticidal cry toxins from *Bacillus thuringiensis* such as 1DLA_A¹³, 1J16_A¹⁴, 3EB7¹⁵, 1CIY_A¹⁶, 2C9K_A¹⁷,

1W99_A¹⁸ and 1I5P_A¹⁹ were submitted to the CLUSTALW²⁰. Output generated by CLUSTALW tool was saved as 'align.phy'. Then the CONSENSE tree for 100 data sets was generated with the help of Phylip²¹. Molecular modeling of TcaA toxin from *Photothabdus luminescens* and Aminopeptidase N from *Helicoverpa armigera*.

TcaA toxin sequence from *Photothabdus luminescens* was submitted to ProDom²² server for detecting the presence of any domains. Templates selection for TcaA and APN were based on the output generated by PSI-BLAST tool²³. To predict the tertiary structure, primary amino residues of these two proteins along with the template suggested by PSI-BLAST tool were submitted to SWISS-MODEL server²⁴ in the alignment mode. As an alternative to homology modeling, threading method was also attempted by accessing the I-TASSER server²⁵. The initial 3D models of the toxins as well as APN were subjected to loop refinement based on the output generated by ERRAT²⁶, ProSA²⁷ and PROCHECK²⁸ server. Loop regions of the proteins showing high percentage of error were further refined through ModLoop server²⁹. After re-validating the refined structures, their structural homologs were searched using the services of DaliLite server³⁰.

Docking studies: Tertiary structures of all domains of TcaA were taken for docking studies with APN receptors from *Helicoverpa armigera* using Hex software³¹. Docked conformations and interaction energies were recorded at the end of the docking exercise. During the dock operation, the total energies were calculated based on shape as well as electrostatics using a default grid spacing of 0.6 Å.

Results and Discussion

Phylogenetic analysis: Phylogenetic analysis of TcaA from *Photothabdus luminescens* was done by including similar group of toxin sequences from other organisms along with Cry toxins of *Bacillus thuringiensis*. The consense tree generated for TcaA toxin branched into two distinct groups, wherein the first group consisted of only Cry toxins from *B. thuringiensis*, while the second group comprised of only TcaA toxins from different species. Further, based on the location of TcaA sequence of *P. luminescens* clade in the consensus tree, it is possible to deduce that, the sequence was evolutionary unrelated to the remaining Cry toxins of *Bacillus thuringiensis*; however, it showed close evolutionary relationship with TcaA toxin of *Burkholderia rhizoxinica* (figure-1).

Molecular modeling studies: The results obtained from ProDom server suggest that TcaA sequence from *Photothabdus luminescens* has six domains (table-1). Although, search for template sequences from PDB using PSI Blast tool did not yield any sequence homologs for any of these 6 domains of TcaA, homologous sequences for the receptor sequence "aminopeptidase N" (APN) from *Helicoverpa armigera* could be retrieved from PDB. Among the various template sequences reported by the PSI Blast tool, human endoplasmic reticulum aminopeptidase which had the maximum sequence identity

(39%) was selected for modeling APN from *H. armigera* (table-2).

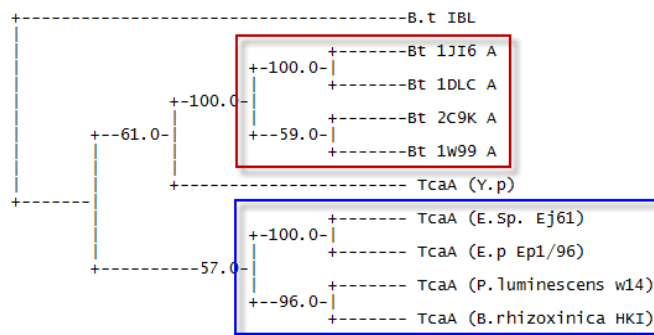


Figure-1
Consensus tree generated for TcaA from *Photothabdus luminescens* using Promlk program of PHYLIP

Table-1
Detection of domains in TcaA sequence from *Photothabdus luminescens* using the ProDom server

Position	ProDom domain	Score E value
1-117	#PD287783	615 5e-63
118-224	#PD156536	555 5e-56
225-595	#PD321543	1989 0
596-836	#PD185778	1296 6e-142
860-999	#PDA1W468	741 1e-77
1000-1095	#PD230859	405 1e-38

The 3D structure of APN from *H. armigera* generated by SWISS MODEL server displayed four domains. While the first (D-I) and third domain (D-III) arranged in sandwich form, consisted of β -sheets (D- I=16; D - III= 6), the fourth (D-IV) domain is made up of α -helices (D-IV=15). The second domain (D-II) had both α -helices (10) and β -sheets (5). Except for minor differences in D-I and D-II, same number of helices / sheets were present in the corresponding domains of the PDB template, 3MDJ_A.

Comparison of homology modeled APN structure of *H. armigera* with crystal structure of human aminopeptidase (3MDJ_A), shows that overall topology of all the four domains (D I, II, III and IV) of the predicted models appears to have more or less similar orientation to that of 3MDJ_A. The second domain (D- II) is having a good sequence homology with the corresponding domain of the crystal structure of human aminopeptidase (3MDJ_A), a catalytic domain determined by Nguyen *et al.* (2011). Therefore, it is possible to speculate similar activity for the theoretical structure of D-II of APN. Sequence analysis revealed that, except for the residue T in the motif "323GATEN327, remaining residues followed by the motif "359HExxHx18E382" of D-II was well conserved with human aminopeptidase 3MDJ_A (figure-2). Methionine located at 267th position of 3MDJ_A was replaced with threonine at the corresponding position of D-II. Studies carried out by Nguyen *et al.* on human aminopeptidase have clearly shown that while "265GAMEN269" motif plays roles in

the exopeptidase specificity of aminopeptidase through motif region “301HEXXH324“ functions as receptors for zinc interaction with the N-terminal amino acid of the substrate, the ligands and are essential for the catalytic activity of the enzyme.

Table-2
Summary of (A) PDB templates generated by PSI blast results and (B) sequence alignment of APN sequence from *Helicoverpa armigera* at the end of 20th iteration

(A)

E-value	BETTER than threshold	Score	E
Sequences producing significant alignments:		(Bits)	Value
pdb 3MDJ A	Chain A, Er Aminopeptidase, Erap1, Bound To The Zi...	1022	0.0
pdb 2YD0 A	Chain A, Crystal Structure Of The Soluble Domain O...	1004	0.0
pdb 3QNF A	Chain A, Crystal Structure Of The Open State Of Hu...	1002	0.0
pdb 3SE6 A	Chain A, Crystal Structure Of The Human Endoplasm...	960	0.0
pdb 3Q7J A	Chain A, Engineered Thermoplasma Acidophilum F3 Fa...	720	0.0
pdb 1Z1W A	Chain A, Crystal Structures Of The Tricorn Interac...	720	0.0

(B)

Query	40	RLPEDLDPINYYVEVTPYFTATDTKEAFTDGLVTTITLRTLKADLNALI IQENVRTINSV	99
		RLPE + P+Y + + T TF G + + T + +I+ + I+	
Sbjct	17	RLPEYVIPVHYDLLIHANLTTL-----TFWGTTKVEI-TASQPTSTIILHSHHLQISRA	69
Query	100	ALTEAGTSVPLHATTPFERITAYHFLKVNLPAGATLENGAVYKLTVDYVGNINETPLSR	159
		L AG + P + + ++ L A L G Y + + Y GN++ET	
Sbjct	70	TLRKGAGERLS---EEPLQVLEHPRQEIALLAPELLVGLPYTVVIHYAGNLSET--FH	124
Query	160	GVFRGSHKDANGNTRWYAATHLQPTNSRQAFPSFDEPGFKSTFDIIINREVTAFPSFSNM	219
		G + + +++ G R A+T +PT +R AFP FDEP FK++F I I R +	
Sbjct	125	GFYKSTYRTKEGELRILASTQFEPTAARMAFPFCDEPAFKASF SIKIRREPRHLAISNMP	184
Query	220	GIKSSDLVNNRIREVFYTTPRMSAYLVTFHISEDFTVIANNNDARSYRILARPTAAGQG	279
		+KS + I + F T +MS YLV F IS+ F ++ + A P Q	
Sbjct	185	LVKSVTVAEGLIEDHFDVTKMSTYLVAFIISD-FESVSKITKSGVKVSVYAVDPKINQA	243
Query	280	QYALEVGPVPTNWLGEYLGIDYYSMDENTNMKNDQIASPYWASGATENWGLVTYRELRL	339
		YAL+ + + +Y I Y K D A P + SGA ENWGL TYRE LL	
Sbjct	244	DYALDAAVTLLEFYEDYF S I P Y-----PLPKQLAAIPDFQSGAMENWGLTTYRESALL	297
Query	340	YQEGETNALDKMYIGTITAHELAHKWFGNLITCRWWDNVWINEGFASYFEYFAMDGVDKT	399
		+ + + + A K + I AHELAH+WFGNL+T WW+++W+NEGFA + E+ ++	
Sbjct	298	FDAEKSASSSKLDITMTVAHELAHQWFGNLVTMEWWDNLWNEGFAKFMFVSVSVTHPE	357
Query	400	MELEDQFNIMYVQSALSADATLSTRALQHTVNSPTEVTGHFSGISYKSGASLLMLKHFL	459
		+++ D F F A+ DA S+ + V +P ++ F +SY KGA +L ML+ +L	
Sbjct	358	LKVGDYFF-GKCFDAMEVDALNSSHPVSTPVENPAQIREMFDDVSYDKGACILNMLREYL	416
Query	460	TENTFKKALNIFLEARKFEHAFPADLFSAFATAVQQDGVF-----S	500
		+ + FK + +L+ +++ DL+ + A+ DGV	
Sbjct	417	SADAFKSGIVQYLQKHSYKNTKNEDLWDSMASICPTDGVKMGDFGFCRSRQSSSSSHWHQ	476
Query	501	NTFDIASFMKYVVEEPGYPVLEVSVNSAAGRIELSKRFLVSATATP-TDQVWPLPLTYT	559
		D+ + M W + G+P++ +V + + Q+ ++ + P T +W +PLT+	
Sbjct	477	ERVDVKTMMNTWTLQRGFPLITITVGR--NVHMKQEHYMKGSDGAPDTGYLWHVPLTFI	534
Query	560	TESNPDWQNLPSKVM TAKTDFIERNVGTNEWVIFNVQQGIYRVNYDTRNWE LLAALS	619
		T + +++ ++ KTD + EW+ FNV G Y V+Y+ W+ L L	
Sbjct	535	TSKS---DMVHRFLKTKTDVLLPEEV-EWIKFNVGMNGYIVHYEDDGDWDLTGLLK	589
Query	620	RDHATAIHLNRAQIVDDVFLMRSGQITRYLGFVKVLDLKKDTSYYSWYPAITGFNWLNR	679
		HTA+ +RA +++ F L+ G+++ + +LK +T P G N L	
Sbjct	590	GHTAVSSNDRASLINNAFQLVSIKLSIEKALDLSLYLKHETE---IMPVFQGLNELIP	646
Query	680	RF-LHLPTTLAAFDIILYGFDAVITDL-GYDVVANE-PLTRILNRFFTLSFACNIGHKG	736
		+ L + + + FL ++ DL +E ++ + R L AC ++	
Sbjct	647	MYKLMKRDNMNEVETQKAFILIRLLRDLIDKQWTWDEGVSERMLRSEL LLLACVHNYQP	706
Query	737	CVDNAVQKRFVAKDNSV--AVNPNLRRHVFCGLRAGGLDEWQYLYNRRQASNNQGDEVA	794
		CV A F K+++ ++ ++ VF G A + W +LY++ Q S + ++	
Sbjct	707	CVQRAEGYFRKWKESGNLSLPVDVTLAVFAVG--AQSTEGWDFLYSKYQFSLSSTESQ	764
Query	795	MLRSLGCTSN TAAGQAYLKMILDDVVKAQDRVNAFFFFYMGRD NAKAGLQFLKDNVDA	854
		+ +L T N Q L D +K Q+ + QFL+ N +	
Sbjct	765	IEFALCRTQNKELQWLLDESFKGDKIKTQE-FPQILTLIGRNPVGYPLAWQFLRKNWNK	823
Query	855	IRKAVVLPWFNN--VLTITAGYLDEAGLRDME---EWWLANQAVPEFAVGISAITSAR	909
		+ + L + V+ TT + L +++ L N + + I I	
Sbjct	824	LVQKFEFGSSSIAHVMGTNTQFSTRTRLEEVKGFSSSLKENGSQLRCVQQTIETI---E	880
Query	910	NNMQWGS DNAATI---IAAANDEDPEDGGSGEE 940	
		N+ W N N I + + E PE +G E	
Sbjct	881	ENIGWMDKNFDKIRVWLQSEKLEHDP EADATGLE 914	

Figure-2

Multiple sequence alignment of Aminopeptidase N from *H. armigera* with selected PDB homologs using ClustalW.



```
3SE6_A      ILNMLKDFLGEEKFQKGI IQYLKFFSYRNAKNDLLWSSLSNSCLESDFTS 443
3Q7J_A      ILRMIEDYAGYEEFRKGISKYLNHDKFGNAEGSDLWTAIEDVS----- 399
gi | 33641859 | gb | AAQ24379.1 | LLLMLKHFLTENTFKKALNIFLEARKFEHAFPADLFSAFATAVQQDGVPS 500
: * * : : : * : : * : : * : : * : :
2YD0_A      MDGFCRSQHSSSSSSHWHQEGVDVKTMMNTWTLQKGFPLITITVGRN-- 489
3QNF_A      MDGFCRSQHSSSSSSHWHQEGVDVKTMMNTWTLQKGFPLITITVGRN-- 489
3MDJ_A      MDGFCRSQHSSSSSSHWHQERVDVKTMMNTWTLQKGFPLITITVGRN-- 489
3SE6_A      GGVCSDPKMSTNMLAFLGENAEVKEMMTTWTLQKGIPLLVVKQDGC-- 491
3Q7J_A      -----GKPVKRVMEYWKNP GPYPVVKLKRNGRK-- 427
gi | 33641859 | gb | AAQ24379.1 | N-----TFDIASFMKYWVEEPGYPVLEVSVNSAAGR 531
: . * * : * * : : .
2YD0_A      VHMKQEHYMKGSD-----GAPDTGYLWHVPLTFITSKS----DMVHRFL 529
3QNF_A      VHMKQEHYMKGSD-----GAPDTGYLWHVPLTFITSKS----DMVHRFL 529
3MDJ_A      VHMKQEHYMKGSD-----GAPDTGYLWHVPLTFITSKS----DMVHRFL 529
3SE6_A      LRLQQRFLQGVFQEDPEWRALQERYLWHIPLTYSTSSS---NVIHRHI 537
3Q7J_A      ITMYQTRFLLNGE-----EEGRWPVPVNIKKK-----DGVGRIL 461
gi | 33641859 | gb | AAQ24379.1 | IELSQKRFLVSAT-----ATPTDQVWPLPLTYTTE SNP DWQNL LPSKV 574
: : * : : . * * : : . : : :
2YD0_A      LKTKTDVLIL-PEEVEWIKFNVGMNGYYIVHYEDDGWDSL TGLLKGHTHA 578
3QNF_A      LKTKTDVLIL-PEEVEWIKFNVGMNGYYIVHYEDDGWDSL TGLLKGHTHA 578
3MDJ_A      LKTKTDVLIL-PEEVEWIKFNVGMNGYYIVHYEDDGWDSL TGLLKGHTHA 578
3SE6_A      LKSKTDLDL-PEKTSWVKFNVD SNGYYIVHYEGHWDLITQLNQHTL 586
3Q7J_A      LEDEAS-----IADGLTKINADSAGFYRVLYDDATFSDVMGHYR----D 502
gi | 33641859 | gb | AAQ24379.1 | MTAKTDFIERNVGTNEWVIFNVQQKGIYRVNVDTRNWE LLAALS RDHTA 624
: : : . : * . * * * : : :
2YD0_A      VSSNDRASLINNAFQLVSI GKLSIEKALDLSLYLKHETEIMPVFQGLNEL 628
3QNF_A      VSSNDRASLINNAFQLVSI GKLSIEKALDLSLYLKHETEIMPVFQGLNEL 628
3MDJ_A      VSSNDRASLINNAFQLVSI GKLSIEKALDLSLYLKHETEIMPVFQGLNEL 628
3SE6_A      LRPKDRVGLIHDVDFQVLAGRLTLDKALDMTYLQHE TSSPALLEGLSYL 636
3Q7J_A      LSPLDRIGLVDDLFAFLLSGHIDPETYRQIRNFFDEDDHNVI TAI V GQM 552
gi | 33641859 | gb | AAQ24379.1 | IHHLNRAQIVDDVFALMRSGQIT YRLGFKVLDFLK KDTSYYSWYPAITGF 674
: : * : : : * : : * : : : : :
2YD0_A      IPMYKLM EKRD MNEVETQFKAF LIRLLRDLIDKQ--TWDEGSVSE RMLR 676
3QNF_A      IPMYKLM EKRD MNEVETQFKAF LIRLLRDLIDKQ--TWDEGSVSE RMLR 676
3MDJ_A      IPMYKLM EKRD MNEVETQFKAF LIRLLRDLIDKQ--TWDEGSVSE RMLR 676
3SE6_A      ESFYHMDRRNISDISENLKRYLLQYFKPVIDRQ--SWSDKGSVSDRMLR 684
3Q7J_A      EYLRMLT--HAFDDDARAFCSRMRQFLTGKQDEN--LKIALGRVSR---- 594
gi | 33641859 | gb | AAQ24379.1 | N--WLRNRFHLHPTTLAAFDE ILYGFLDAVITDLGYDVVANEPLR TLNR 722
: : : :
2YD0_A      SLLLLLACVHNYQPCVQRAEGYFRKWKESNGNLSLPVDVTLAVFAVGAQS 726
3QNF_A      SLLLLLACVHNYQPCVQRAEGYFRKWKESNGNLSLPVDVTLAVFAVGAQS 726
3MDJ_A      SLLLLLACVHNYQPCVQRAEGYFRKWKESNGNLSLPVDVTLAVFAVGAQS 726
3SE6_A      SALLKLCADLNHAPCIQAAELFSQWMESSGKLNIP TDVLKIVYSVGAQT 734
3Q7J_A      -----LYVMVDESYAEEMSKLFD SAEP-----EMRSSIATAVALV 632
gi | 33641859 | gb | AAQ24379.1 | FFTLSFACNIGHKGCVDNAVQKFVALKDNSVAVNPNLRRHVFCEGLRAGG 772
: . * : : . : : : :
2YD0_A      TEGWDFLYSKYQFSL SSTEKSQIEFALCRTQNK EKQLWLLDESFKGDKIK 776
3QNF_A      TEGWDFLYSKYQFSL SSTEKSQIEFALCRTQNK EKQLWLLDESFKGDKIK 776
3MDJ_A      TEGWDFLYSKYQFSL SSTEKSQIEFALCRTQNK EKQLWLLDESFKGDKIK 776
3SE6_A      TAGWNYLLEQYELSMSSAEQNKILYALSTSKHQEKLLKLIELGMGEKVIK 784
3Q7J_A      TGD LKGLLEKFRSVD RDEDRVRIISAFGK LKSNTDLS TVYGMVEKTEIKK 682
gi | 33641859 | gb | AAQ24379.1 | LDEWQYLYNRRQASNNQGEVAMLRSLGCTSNTAAGQAYLKMILDDVVVK 822
. * : : . : : : : *
2YD0_A      TQ-EFPQILTLIGRNPVGYPLAWQFLRKNWNKLVQK FELGSSSIAHMVMG 825
3QNF_A      TQ-EFPQILTLIGRNPVGYPLAWQFLRKNWNKLVQK FELGSSSIAHMVMG 825
3MDJ_A      TQ-EFPQILTLIGRNPVGYPLAWQFLRKNWNKLVQK FELGSSSIAHMVMG 825
3SE6_A      TQ-NLAALLHAIARRPKGQQLAWDFVRENWTHLLKFFDLGSYDIRMISG 833
3Q7J_A      QD-MISFSSALETLP-----GREFIFANLDRIRLVI----- 714
gi | 33641859 | gb | AAQ24379.1 | AQDVRVNAFFSYFMGHRDNKAGLQFLKDNVDAIRKAVVLP--AWFN NVLT 870
: . : : : * : : .
2YD0_A      TTNQFSTRTRLEE VKGFFSSLKENGSQLRCVQQT IETIEENIGWMDKNFD 875
3QNF_A      TTNQFSTRTRLEE VKGFFSSLKENGSQLRCVQQT IETIEENIGWMDKNFD 875
3MDJ_A      TTNQFSTRTRLEE VKGFFSSLKENGSQLRCVQQT IETIEENIGWMDKNFD 875
3SE6_A      TTAHFSSKDKLQEVKLFESLEAQGSHLDIFQTVLETITKNIKWLEKNLP 883
3Q7J_A      -----
gi | 33641859 | gb | AAQ24379.1 | TTAGYLDEAGLRDMEWLLANQNAVPEFAVGISAIT SARNNMQWGS DNAA 920
```

A large cavity was observed between D-II and D-IV of APN model which had resemblance to the template 3MDJ_A. Based on this, it is hypothesized that this cavity could provide an easy access to the catalytic site for substrates and might also represent binding site for peptide based substrates³². The D-III is the smallest among all the domains and act as a connecting domain between D-II and D-IV (Figure-3A). Superimposition of C α backbone of predicted model onto 3MDJ_A shows very low RMSD value of 1.1Å.

I-TASSER software was successful in predicting the 3D structures for all the six domains of TcaA from *Photothabdus luminescens* (Figure-3B). Among these six domains D-I, II, V and VI are purely made up of α -helices (D-I=6, D-II=4, D-V=9 and D-VI =5). Helices of D-II are arranged as antiparallel helix-loop-helix motif in a manner similar to that of solution NMR structure of metalloprotein from *Escherichia coli* (PDB ID: 2HZ8) determined by Calhoun *et al* (2008)³³. However, both D-III and D-IV had α -helices (D-III=11 and D-IV= 15) as well β -sheets (D III = 5 and D IV= 2). While the folding pattern of D-III is like a horseshoe comparable to that of the crystal structure of ribonuclease inhibitor (PDB ID 2BEX)³⁴, D-IV architecture resembled to a half-doughnut which is identical to the crystal structure of mitochondrial transcription termination factor 3 from human (PDB ID: 3M66)³⁵. Superimposition of C α backbone of all these structures onto the top PDB template used by I-TASSER showed a very low RMSD (table-3).

Table-3

RMSD of all the six domains of TcaA from *Photothabdus luminescens* generated by the Dali server

Domains	Templates used by I-TASSER	RMSD generated by DALI server
Domain I	3V42_A	2.2
Domain II	2HZ8_A	1.5
Domain III	2BEX_A	2.6
Domain IV	3M66_A	1.9
Domain V	2J00_A	3.1
Domain VI	3KPH_B	3.3

Structure validation: Validation of the theoretical models of TcaA and APN by the structural assessment tools such as ProSA, ERRAT and PROCHECK showed that there was an improvement in the quality of the predicted structure upon loop refinement. Quality factor of the loop refined APN model calculated by ERRAT reached 57.65 from 48.941. The Z score value computed by the ProSA tool for APN model was -8.89. This suggests that the models are lying within the Z score values of native conformational structures. Ramachandran plot generated by PROCHECK indicates that most of the residues from APN model have ϕ and ψ angles in the core and allowed regions. This indicates that most of the main-chain conformations of models are consistent with their side-chain conformations. Summary of the Ramachandran plot revealed that, 85.5% of the residues of APN structure were distributed in

the core region, followed by 12.8% in the allowed, 1.0% in the general and remaining 0.9% in the disallowed. The overall G-score calculated for APN model was found to be -0.08 which was above the threshold value indicating the predicted model was satisfactory.

Improvement in the quality of the structure upon loop refinement was also seen in all the six TcaA domains of *Photothabdus*. The Φ and ψ angles of these theoretical models were present in the core and allowed region. Ramachandran plot statistics indicates that the predicted models were of good quality (table-4).

Table-4

PROCHECK summary for all the seven domains of TcaA from *Photothabdus luminescens*

Domains	Residues Present in				G-factor
	Core region	Allowed region	General region	Disallowed region	
I	84.8%	11.4%	1.9%	1.9%	-0.05
II	90.8%	9.2%	0.0%	0.0%	0.01
III	68.8%	25.0%	3.1%	3.1%	-0.49
IV	84.8%	10.1%	3.2%	1.8%	-0.06
V	82.8%	12.5%	3.1%	1.6%	-0.18
VI	87.4%	9.2%	1.1%	2.3%	0.15

Docking studies: HEX was successful in docking the homology modeled aminopeptidase receptor of *Helicoverpa armigera* on to all the six domains of TcaA toxin model of *Photothabdus luminescens*. Based on the docking energies for all the six domains of TcaA presented in table 5, the D-I model got docked onto the APN receptor model with the highest dock energy of -792.9 KJ / mol. Visualization of the docked output using DeepView package reveal that a total of 121 residues of both D-I domain and APN model are involved in the interaction (D-I = 59 and APN = 62 residues) (figure-4). Among these 121 residues, maximum residues are non polar in nature (table-6) (figure-5). The docked complex was stabilized by the formation of strong inter-molecular hydrogen bonds.

Table-5

Summary of the docking energy of APN from *Helicoverpa armigera* onto the different domains of TcaA from *Photothabdus luminescens*

Domains	Binding energy with APN from <i>Helicoverpa armigera</i>
I	-792.9 kj/mol
II	-719.0 kj/mol
III	-304.1 kj/mol
IV	-274.9 kj/mol
V	-588.5 kj/mol
VI	-656.8 kj/mol

Conclusion

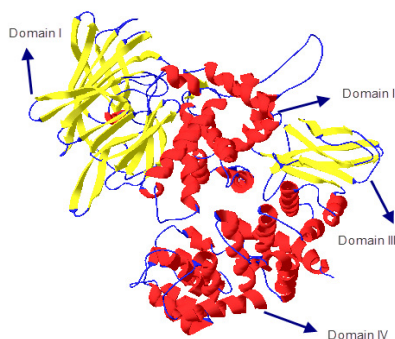
Based on the *in-silico* studies conducted on the interaction of TcaA toxin from *Photorhabdus luminescens* with the aminopeptidase N receptor of *Helicoverpa armigera* we can

conclude that TcaA toxin can be considered as a potential biopesticide for controlling the pest population affecting the agricultural crops.

Table-6
Summary of residues interacting between DI of TcaA and homology modeled APN receptor from *Helicoverpa armigera*

Acidic	Basic	Polar	Non Polar
DI of TcaA			
asp30,97,106,108,111, glu63,77,101	lys8,66,81,85, arg36,61,70,75,115	gln6,26,41,60,73,76,89, asn7,64,91, ser10,33,67,90,117, tyr25	val14,28,40,94, met5,113, ile9,34, phe11,109, ala37,71,98,116, gly24,105,107 leu65,68,74,86,89,95,112, trp72, pro78
APN receptor (<i>Helicoverpa armigera</i>)			
asp780, glu109,390,841	lys812, arg118,289,752,781, his121,394,	gln367,779, asn108,806,783, ser113,120,277,396,399,786, thr29, 110,389,362, tyr274,307,400	val54,748,782,814,815 met364,790, ile363,398,810 phe395,787,802,820 ala276,372,778,813,818 gly26,119,278,393,397 leu112,291,751,816 trp130,275,631,842 pro111

(A)



(B)

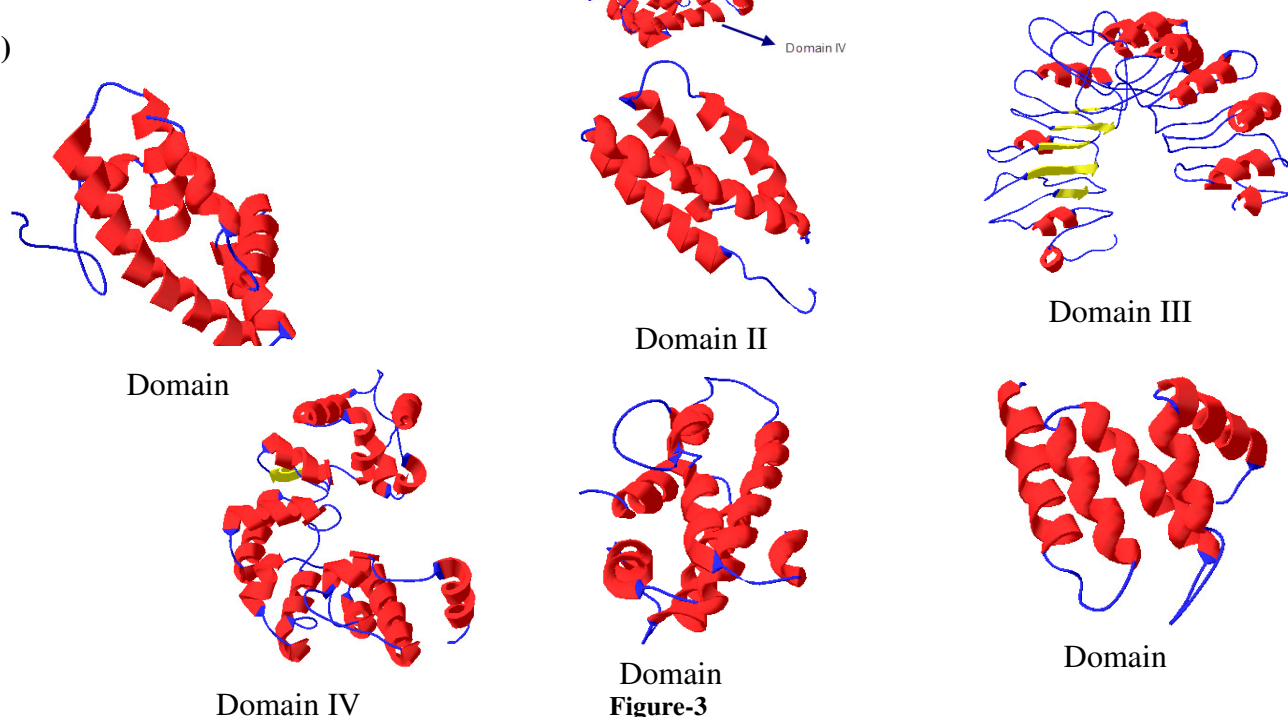


Figure-3
 3D structure of (A) APN receptor from *Helicoverpa armigera* (B) TcaA toxin from *Photorhabdus luminescens*

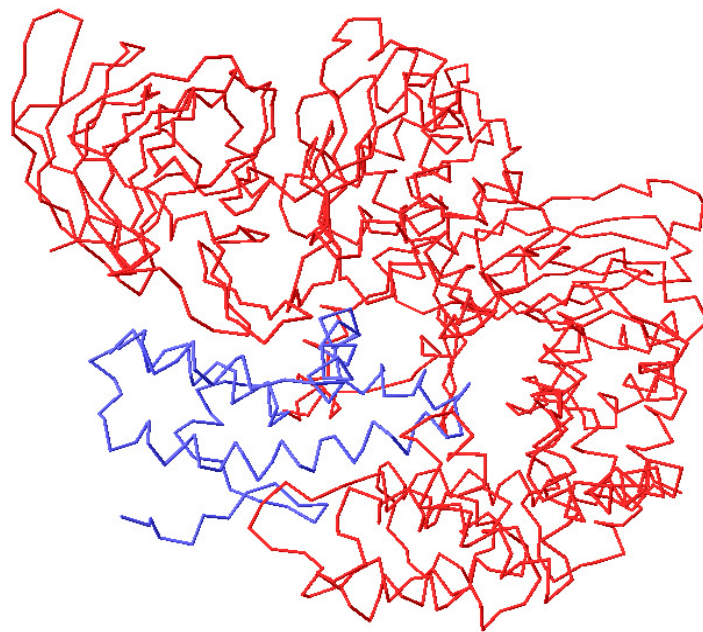


Figure-4

Docking of D-I of TcaA onto homology modeled aminopeptidase N from *Helicoverpa armigera* using HEX software (Total energy = -792.9 KJ / mol)

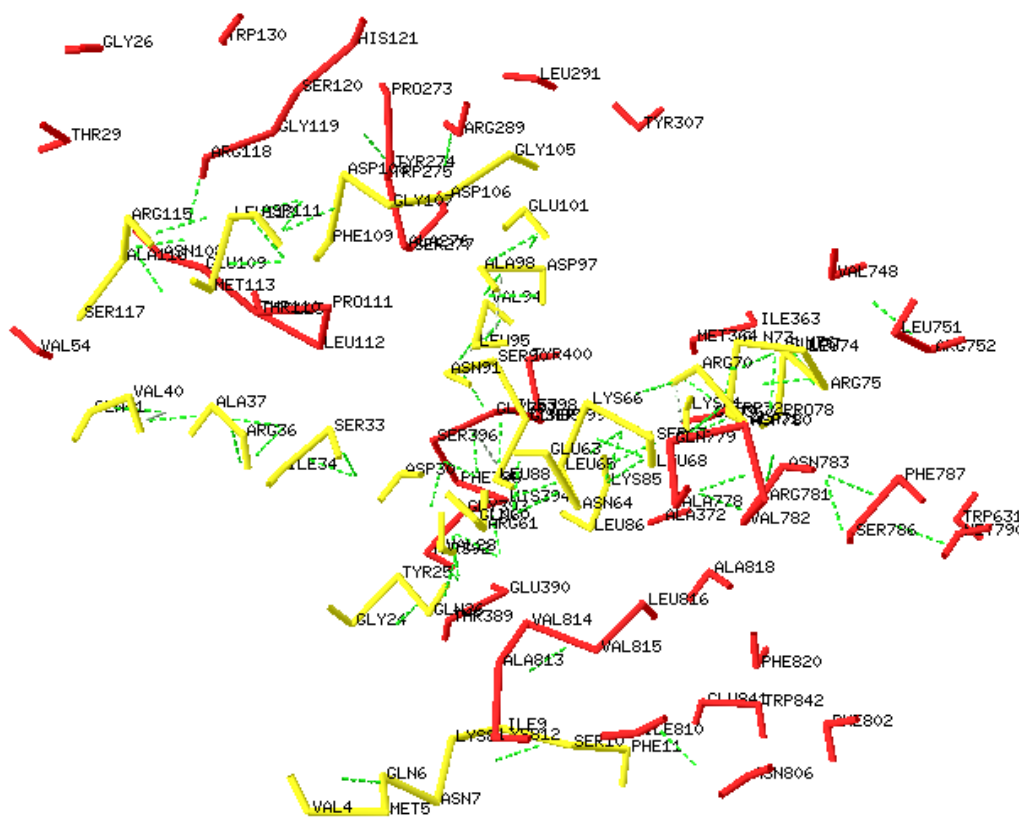


Figure-5

Amino acid residues of TcaA of *Photobacterium luminescens* (Yellow) interacting with homology modeled aminopeptidase N receptor from *Helicoverpa armigera* (Red) within 5 Å distance.

References

1. Roush R., Can we slow adaptation by pests to insect transgenic crops? In: Parsley GJ (ed) Biotechnology and integrated pest management. CAB International, Willinford. (1996)
2. Poinar G. O, Thomas G. M. and Hess R., Characteristics of the specific bacterium associated with Heterorhabditis bacteriophora (Heterorhabditidae: Rhabditida), *Nematologica.*, **23**, 97–102 (1977)
3. Wirth M. C., Georghiou G. P., and Federici, B. A., Cyt A enables CryIV endotoxins of BT to overcome high levels of CryIV resistance in the mosquito, *Culex quinquefasciatus*, *Proc. Natl. Acad. Sci.*, **94**, 10536-10540. (1997)
4. Gould F. Anderson A. Jones A. Sumerford D. Heckel D. Lopez, J., et al. Initial frequency of alleles for resistance to *Bacillus thuringiensis* toxins in field populations of *Heliothis virescens*. *Proc. Natl. Acad. Sci.*, **94**, 3519-3523(1997)
5. Liu Y. B. Tabashnik B. Dennehy T. Patin A. and Bartlet A., Development time and resistance to Bt crops, *Nature*, **400**, 519 (1999)
6. Frutos R. Rang C. and Royer M., Managing Insect Resistance to Plants Producing *Bacillus thuringiensis* Toxins, *Crit. Rev. Biotechnol.*, **19**(3), 227-276 (1999)
7. Tabashnik B., Delaying Insect Adaptation to Transgenic Plants: Seed Mixtures and Refugia Reconsidered, *Proc. R. Soc. Lond.*, **255**(1342), 7-12 (1994)
8. Blackburn M. Golubeva E. Bowen D. and Ffrench-Constant R., A novel insecticidal toxin from *photorhabdus luminescens*, toxin complex a (Tca), and its histopathological effects on the midgut of *manduca sexta*, *Applied and environmental microbiology*, **64**(8), 3036-3041(1998)
9. Han R. and Ehlers R. U., Effect of *Photorhabdus luminescens* phase variants on the in vivo and in vitro development and reproduction of the entomopathogenic nematodes *Heterorhabditis bacteriophora* and *Steinernema carpocapsae*, *FEMS microbiology ecology*, **35**(3), 239-247 (2001)
10. Knight P. J. Crickmore N. Ellar D. J., The receptor for *Bacillus thuringiensis* CryIA(c) delta-endotoxin in the brush border membrane of the lepidopteran *Manduca sexta* is aminopeptidase N, *Mol. Microbiol* **11**, 429–436 (1994)
11. Francis B. R. and Bulla Jr L. A., Further characterization of BT-R1, the cadherin-like receptor for CryIAb toxin in tobacco hornworm (*Manduca sexta*) midguts, *Insect Biochem. Mol. Biol.*, **27**, 541–550 (1997)
12. Knight P. J. Carroll J. and Ellar D. J., Analysis of glycan structures on the 120 kDa aminopeptidase N of *Manduca sexta* and their interactions with *Bacillus thuringiensis* Cry1Ac toxin, *Insect Biochem. Mol. Biol* **34**, 101–112 (2004)
13. Li J. D. Carroll J. and Ellar D. J. Crystal structure of insecticidal delta-endotoxin from *Bacillus thuringiensis* at 2.5 Å resolution, *Nature*. **353**, 815-821 (1991)
14. Galitsky N. Cody V. Wojtczak A. Ghosh D. Luft J. R. Pangborn W. and English L., Structure of the insecticidal bacterial delta-endotoxin Cry3Bb1 of *Bacillus thuringiensis*, *Acta crystallogr D Biol Crystallogr* **57**, 1101-1109 (2001)
15. Guo S. Ye S. Liu Y. Wei L. Xue J. Wu H. Song F. Zhang J. Wu X. Huang D. Rao Z., Crystal structure of *Bacillus thuringiensis* Cry8Ea1: An insecticidal toxin toxic to underground pests, the larvae of *Holotrichia parallela*, *J struct Biol* , **168**, 259-266 (2009)
16. Grochulski P. Masson L. Borisova S. Pusztai-Carey M. Schwartz J. L. Brousseau R. Cygler M., *Bacillus thuringiensis* CryIA(a) insecticidal toxin: crystal structure and channel formation, *J Mol Biol.* **254**, 447-464 (1995)
17. Boonserm P. Mo M. Angsuthanasombat C. and Lescar J., Structure of the functional form of the mosquito larvicidal Cry4Aa toxin from *Bacillus thuringiensis* at a 2.8-angstrom resolution, *J Bacteriol.* **188**, 3391-3401 (2006)
18. Boonserm P. Davis P. Ellar D. J. and Li J., Crystal structure of the mosquito-larvicidal toxin Cry4Ba and its biological implications, *J Mol Biol.* **348**, 363-382 (2005)
19. Morse R. J. Yamamoto T. and Stroud R. M., Structure of Cry2Aa suggests an unexpected receptor binding epitope, *Structure* **9**, 409-417 (2001)
20. Thompson J. D. Higgins D. G. and Gibson T. J., CLUSTAL W: improving the sensitivity of progressive multiple sequence alignment through sequence weighting, position-specific gap penalties and weight matrix choice, *Nucleic Acids Res* , **22**, 4673-4680 (1994)
21. Felsenstein J. *Inferring phylogeny*, Sinauer Associates, Sunderland, MA (2003)
22. Servant F.C. Bru E. Courcelle J. Gouzy D. Peyruc D. and Kahn D., ProDom: Automated clustering of homologous domains, *Briefings in Bioinformatic*, **3**, 246-251(2002)
23. Altschul S. F. Madden T. L. Schäffer1 A. A. Zhang J. Zhang Z. Miller W. and Lipman D. J., Gapped BLAST Nucleic Acids Res and PSI-BLAST: a new generation of protein database search programs, *Nucleic Acids Res*, **17**, 3389-3402 (1997)

24. Schwede T. Kopp J. Guex N. and Peitsch M. C., SWISS-MODEL: an automated protein homology-modeling server, *Nucl. Acids Res*, **31**, 3381-3385 (2003)
25. Zhang Y., I-TASSER server for protein 3D structure prediction, *BMC bioinformatics*, **9**, 40-47 (2008)
26. Colovos C. and Yeates T. O., Verification of protein structures: Patterns of nonbonded atomic interactions, *Protein Science*, **2**, 1511-1519 (1993)
27. Wiederstein M. and Sippl M. J., ProSA-web: interactive web service for the recognition of errors in three-dimensional structures of proteins, *Nucleic Acids Res* , **35**, W407-W410 (2007)
28. Laskowski R. A. MacArthur M. W. Moss D. and Thornton J. M., PROCHECK: a program to check the stereochemical quality of protein structures, *J. Appl. Cryst*, **26**, 283-291(1993)
29. Fiser A. Do R. K. and Sali A. Modeling of loops in protein structures. *Protein Science* **9**, 1753-1773(2000)
30. Holm L. and Rosenstrom P. Dali server: conservation mapping in 3D, *Nucl Acids Res* **38**, 545-549 (2010)
31. Ritchie D. W., Evaluation of protein docking predictions using Hex 3.1 in CAPRI rounds 1 and 2. *Proteins, Structure, Function, and Bioinformatics*, **52**, 98-106 (2003)
32. Nguyen T. T. Chang S. Evnouchidou I. York I. A. et al., Structural Basis For Antigenic Peptide Precursor Processing by the Endoplasmic Reticulum Aminopeptidase ERAP1, *Nat Struct Mol Biol*. **18**, 604-613 (2011)
33. Calhoun J. R. Liu W. Spiegel K. et al., Solution NMR Structure of a Designed Metalloprotein and Complementary Molecular Dynamics Refinement, *Structure* **16**, 210-215 (2008)
34. Iyer S. Holloway D. E. Kumar K. Shapiro R. and Acharya K. R., Molecular Recognition of Human Eosinophil-derived Neurotoxin (RNase 2) by Placental Ribonuclease Inhibitor, *J. Mol. Biol*. **347**, 637-655 (2005)
35. Spahr H. Samuelsson T, Hällberg B. M. and Gustafsson C. M., Structure of mitochondrial transcription termination factor 3 reveals a novel nucleic acid-binding domain, *Biochem. Biophys. Res. Commun*. **397**, 386-390 (2010)